



Solution NMR assignment of the ARC4 domain of human tankyrase 2

Mariola Zaleska¹ · Katie Pollock^{1,2} · Ian Collins² · Sebastian Guettler¹ · Mark Pfuhl³ 

Received: 8 February 2019 / Accepted: 2 March 2019
© The Author(s) 2019

Abstract

Tankyrases are poly(ADP-ribose)polymerases (PARPs) which recognize their substrates via their ankyrin repeat cluster (ARC) domains. The human tankyrases (TNKS/TNKS2) contain five ARCs in their extensive N-terminal region; of these, four bind peptides present within tankyrase interactors and substrates. These short, linear segments, known as tankyrase-binding motifs (TBMs), contain some highly conserved features: an arginine at position 1, which occupies a predominantly acidic binding site, and a glycine at position 6 that is sandwiched between two aromatic side chains on the surface of the ARC domain. Tankyrases are involved in a multitude of biological functions, amongst them Wnt/ β -catenin signaling, the maintenance of telomeres, glucose metabolism, spindle formation, the DNA damage response and Hippo signaling. As many of these are relevant to human disease, tankyrase is an important target candidate for drug development. With the emergence of non-catalytic (scaffolding) functions of tankyrase, it seems attractive to interfere with ARC function rather than the enzymatic activity of tankyrase. To study the mechanism of ARC-dependent recruitment of tankyrase binders and enable protein-observed NMR screening methods, we have as the first step obtained a full backbone and partial side chain assignment of TNKS2 ARC4. The assignment highlights some of the unusual structural features of the ARC domain.

Keywords ADP-ribosylation · Ubiquitylation · Ankyrin repeats · Signaling

Biological context

The tankyrases (TNKS/ARTD5, TNKS2/ARTD6) are poly(ADP-ribose)polymerases (PARPs) and as such catalyse the processive modification of protein substrates with poly(ADP-ribose) (PAR) chains, thereby consuming their co-substrate NAD⁺ (Haikarainen et al. 2014). PARPs are part of a larger family of Diphtheria-toxin-like ADP-ribosyltransferases (ARTDs), which share variants of a conserved catalytic domain that either modifies substrates with mono-ADP-ribose or PAR, or lacks detectable catalytic activity (Hottiger et al. 2010; Vyas et al. 2014). Different ARTD family members are distinguished by unique combinations

of accessory domains, which confer functional diversity (Hottiger et al. 2010). In the case of the tankyrases, these are an extensive N-terminal region comprising five consecutive ankyrin repeat clusters (ARCs), either flexibly or rigidly linked, and responsible for substrate recruitment (Seimiya et al. 2004; Guettler et al. 2011; Eisemann et al. 2016). The ARCs are followed by a polymerizing sterile alpha motif (SAM) domain (De Rycker and Price 2004; Mariotti et al. 2016; Riccio et al. 2016) that precedes the PARP domain (Lehtiö et al. 2008). ARCs and the SAM domain direct tankyrase to regulators of a wide range of biological processes, among which Wnt/ β -catenin signaling (Huang et al. 2009; Mariotti et al. 2016, 2017; Yang et al. 2016), the maintenance and mitotic resolution of telomeres (Smith et al. 1998; Smith and de Lange 2000; Dynek and Smith 2004) and glucose metabolism (Chi and Lodish 2000; Yeh et al. 2007; Zhong et al. 2016) are some of the best-studied. Additional roles of tankyrase include the regulation of mitotic spindle formation (Chang et al. 2005, 2009), Hippo signaling (Wang et al. 2015; Troilo et al. 2016; Jia et al. 2017) and emerging functions in the DNA damage response (Nagy et al. 2016), cell migration (Lupo et al. 2016), and Notch signaling (Bhardwaj et al. 2017), to name a few. Proteomics

✉ Mark Pfuhl
mark.pfuhl@kcl.ac.uk

¹ Divisions of Structural Biology & Cancer Biology, The Institute of Cancer Research (ICR), London SW7 3RP, UK

² Division of Cancer Therapeutics, The Institute of Cancer Research (ICR), London SW7 3RP, UK

³ School of Cardiovascular Medicine and Sciences and Randall Centre, King's College London, Guy's Campus, London SE1 1UL, UK

NOESY-HSQC experiments recorded at 700 and 800 MHz on Bruker Avance spectrometers at 20 °C. Spectra were processed with Topspin 3.1 (Bruker), and all assignments were performed with CCPN analysis 2.4 (Vranken et al. 2005).

Assignments and data deposition

The TNKS2 ARC4 domain construct comprises 165 amino acids (residues 488–649 plus 3 additional N-terminal amino acids, GAM, resulting from the cloning method) and despite its substantial molecular weight of 17.8 kDa gives excellent NMR spectra (see Fig. 1). It was possible to find assignments for 164 residues with only the N-terminal glycine missing completely. Of the assigned residues, backbone amide peaks were missing for only two of the non-proline residues (R525 and V584). Out of a total of 165 backbone nitrogens, 165 α carbons, 151 β carbons, 140 γ carbons, 99 δ carbons, 31 ϵ carbons and 165 backbone carbonyls, a total of 156 (94.5%), 163 (98.7%), 148 (98.0%), 68 (48.6%), 42 (42.4%) and 11

(35.4%), respectively, could be assigned. The assignment has been deposited with the BMRB, accession code 27747.

Comparison to X-ray structure

The NMR spectra of ARC4 contain a number of unusual features, most prominently the appearance of 3 peaks for histidine sidechain $N\epsilon_2/H\epsilon_2$ groups, two of which could be assigned. Such resonances are usually exchange-broadened beyond detection. ARC4, however, makes a rather unusual use of histidines as part of the conserved ankyrin repeat (AR) infrastructure, with regular occurrences at the N-terminal end of the first helix and the C-terminal end of the second helix of each AR. Thus, they appear on opposite sides of the protein in the central three ARs (see Fig. 2). Those at the C-termini of the second helix point into solution whereas those at the N-termini of the first are covered by the long loop/beta hairpins which connect adjacent ARs. The latter are part of a highly conserved TPLH sequence motif (Mosavi et al. 2002). As part of this motif, the histidine He2 acts as an H-bond donor to the backbone carbonyl group of the residue preceding the TPLH motif in the following repeat (Preimesberger et al. 2015). Our observation of three histidine sidechain $N\epsilon_2/H\epsilon_2$ groups is therefore in good agreement with the structure. Curiously, the C_α secondary shifts of two of these three protected histidines (H531 with almost 9 ppm, H564 with almost 10 ppm; H597

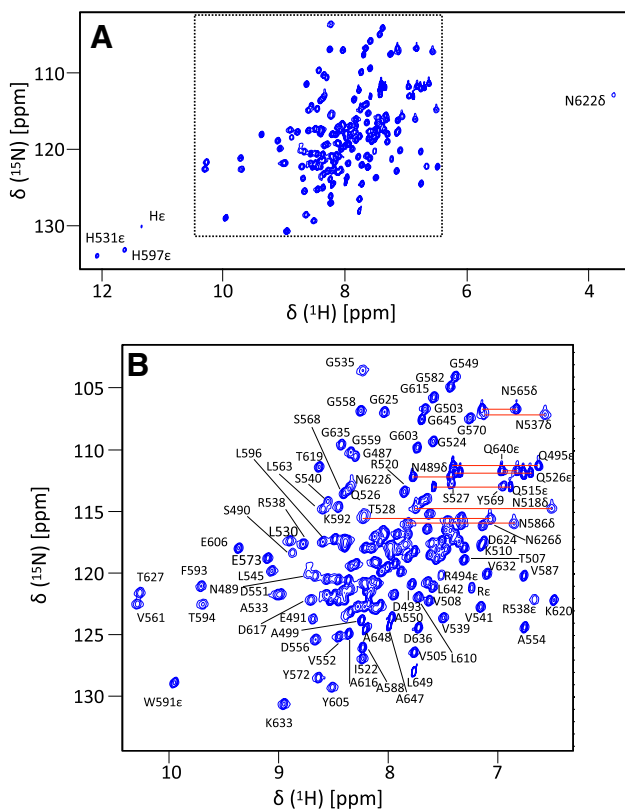


Fig. 1 ^1H - ^{15}N HSQC spectrum of 1 mM uniformly $^{15}\text{N}/^{13}\text{C}$ labelled ARC4 recorded at a temperature of 293 K and a field of 700 MHz. Note that the sidechain resonances of histidines and arginines are folded from their original position in the ^{15}N dimension. **a** Overview spectrum. **b** Majority of the backbone resonances in the spectrum (indicated by box in **a**). Well resolved peaks have been labelled with their assignments; pairs of peaks for sidechain NH_2 groups are connected by red lines

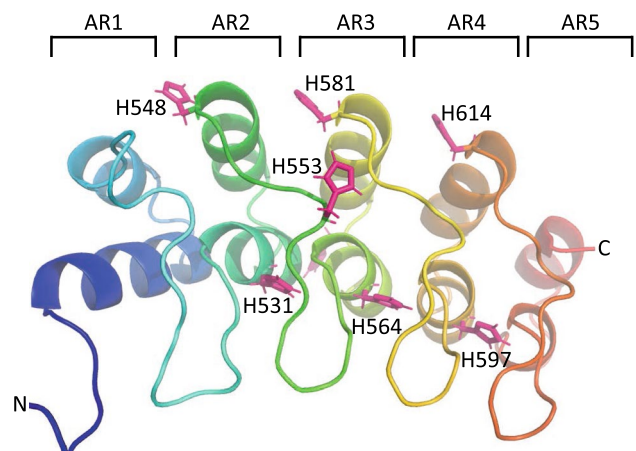


Fig. 2 Structure of ARC4 (PDB code 3TWQ) showing all histidine side chains as sticks in pink while the main backbone is shown in cartoon style coloured by sequence from N-terminus (blue, left) to C-terminus (red, right). Ankyrin repeats (ARs) are numbered AR1 to AR5. The positions of the histidines occupying key positions in the three central ARs are clearly visible with H548, H581 and H614 pointing towards the solvent (top) while H531, H564 and H597 (bottom) are covered by the β -hairpins linking ARs. H553 (front) and H571 (back, not labelled) are not part of the conserved AR pattern and exposed to solvent

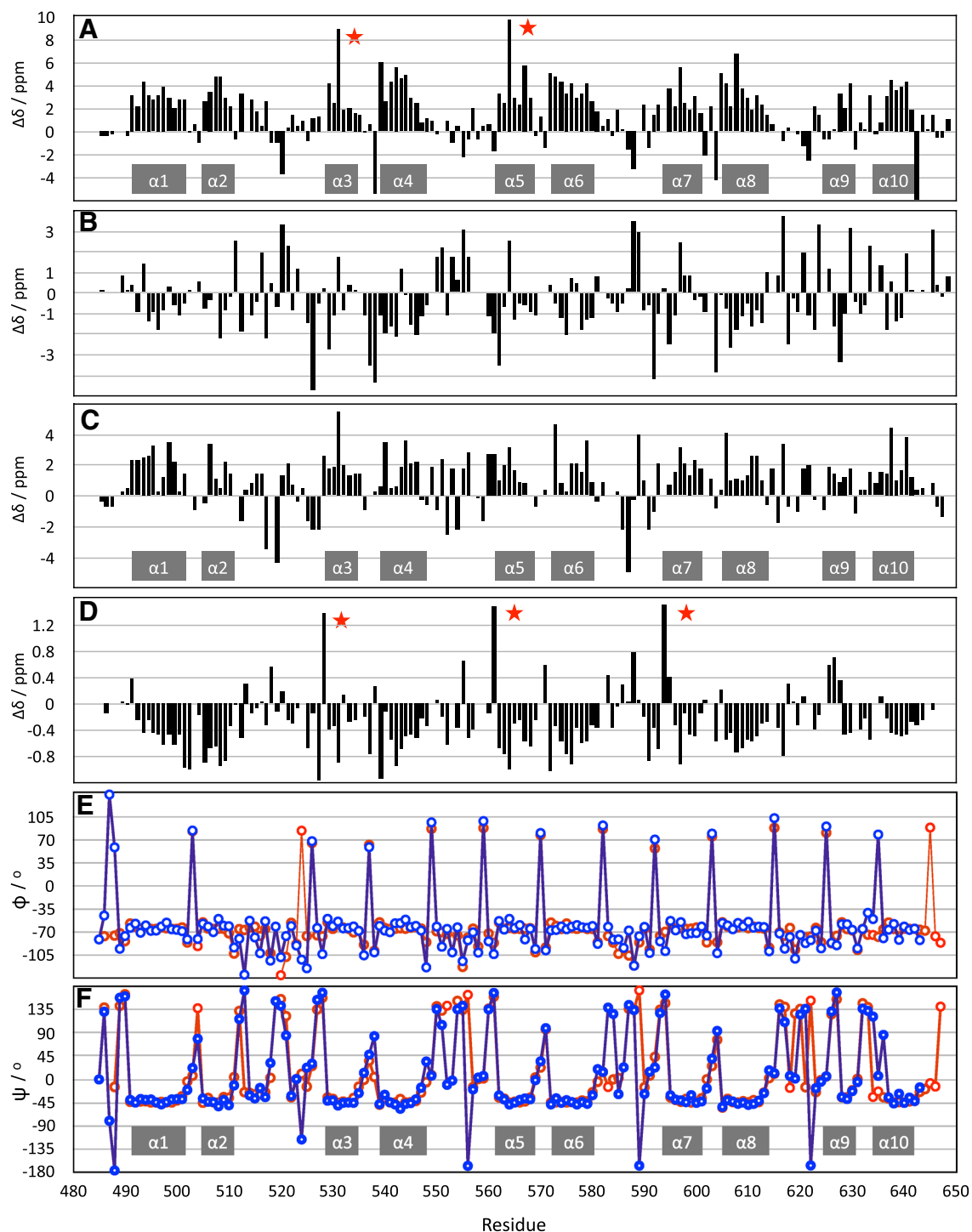


Fig. 3 Secondary chemical shifts (Wishart and Sykes 1994) and backbone dihedral angles predicted from Dangle and extracted from the crystal structure of ARC4 (PDB code 3TWQ) (Guettler et al. 2011) All values were calculated using CCPN analysis version 2.4, and figures were generated in Apple Numbers, inkscape and keynote.

a $C\alpha$, **b** $C\beta$, **c** C' , **d** $H\alpha$, **e** phi, **f** psi. Dihedral angles from Dangle are shown in red, those from the crystal structure in blue. Positions of secondary structure elements based on the chemical shift analysis are indicated as grey bars. Positions of the protected histidines with chemical shift outliers are indicated by red stars

with 5.5 ppm is less extreme but still substantial) are well outside the $[-5.0, +5.0]$ bracket of all the other residues (see Fig. 2). This pattern is less apparent for the $C\beta$ and

C' secondary shifts. However, it is repeated, albeit with a shift of -3 in the sequence, for the $H\alpha$ secondary chemical shifts: residues T528, V561 and T594 have values of around

+ 1.4, much larger than all the other values, which are well within the $[-0.8, +0.8 \text{ ppm}]$ bracket. It is not completely clear what causes the unusual chemical shifts. The fact that these instances of unusual secondary chemical shifts occur in precisely repeated structural units in AR–AR boundaries suggests that the most unusual backbone conformation, in combination with the hydrogen bonds from the histidine side chains to the backbone amides i-3 (Preimesberger et al. 2015), are likely to be the causative factor.

Another unusual feature is the sidechain amide group of N622, which has proton resonances at 8.33 and 3.59 ppm. The extreme shift of one of the amides can be explained by its position extremely close to the aromatic ring of F593, with which it is very likely to form a π –hydrogen bond.

Finally, we can observe three arginine sidechain $\text{N}\epsilon$, which is also not common at pH values around 7. Two of these could be assigned to R538 and R494. R494 is very likely involved in simultaneous salt bridges with the neighbouring E491 and E523 (shortest distances from R494H η 11–E491 O ϵ 2: 2.0 Å; R494H ϵ –E523 O ϵ 2: 3.0 Å). The H ϵ of R538 is likely to make a hydrogen bond to the backbone carbonyl oxygen of K501 (distance R538 H ϵ –K501 O': 2.0 Å).

Secondary structure

We analysed the secondary structure of ARC4, based on the backbone chemical shifts, and compared it to the crystal structure (Guettler et al. 2011) (PDB code 3TWQ). In the first instance, we qualitatively compared the positions of the helices; we next quantitatively compared the backbone dihedral angles predicted by Dangle (Cheung et al. 2010) to those extracted from the crystal structure (see Fig. 3). The positions of the helices are generally in good agreement with the individual secondary chemical shifts, especially the C_α and H_α values, while C' and C_β provide a less clear correlation. The only exception is helix 9 where some values for H_α deviate somewhat. Even more intriguing is the result of the Dangle analysis. We can see an excellent agreement of the values with those from the crystal structure. Most importantly, the sharp changes of phi and psi between the helices are precisely matched for most residues. (Note the apparently huge difference in psi prior to the first helix of each AR (H1, H3, H5, H7, H9), which is actually very small due to the circular periodicity of the dihedral value; i.e., a value of $+175^\circ$ is actually very close to -175° .) The only deviations are seen prior to helix 3, near to H531 and at the C-terminus. The region around the former folds in an unusual way and involves rare interactions which cause unusual chemical shifts as outlined above. At the latter, the conformation is less well defined and likely to differ between solution and crystal. We can therefore conclude that for a protein with a low level of conformational dynamics, and thus a very

narrow distribution of conformations in solution and in the crystal, we can extract very precise backbone dihedral angle constraints.

Acknowledgements Work in the SG laboratory is funded by The Institute of Cancer Research (ICR), by Cancer Research UK through a Career Establishment Award to SG (C47521/A16217) and by the Lister Institute of Preventive Medicine. Work in the IC laboratory is supported by ICR and Cancer Research UK through funding to the Cancer Therapeutics Unit (C309/A11566). KP was supported by a Wellcome Trust Ph.D. studentship (WT102360/Z/13/Z). SG and IC acknowledge funding through a Faringdon Proof of Concept Fund Award from ICR. NMR spectra were recorded in the King's College London Centre of Biomolecular Spectroscopy and at the MRC Biomolecular NMR Centre based at the Francis Crick Institute. The authors wish to thank Andrew Atkinson and Geoff Kelly for help with recording the spectra and Maggie Liu for initial NMR work and advice.

Open Access This article is distributed under the terms of the Creative Commons Attribution 4.0 International License (<http://creativecommons.org/licenses/by/4.0/>), which permits unrestricted use, distribution, and reproduction in any medium, provided you give appropriate credit to the original author(s) and the source, provide a link to the Creative Commons license, and indicate if changes were made.

References

- Bhardwaj A, Yang Y, Ueberheide B, Smith S (2017) Whole proteome analysis of human tankyrase knockout cells reveals targets of tankyrase-mediated degradation. *Nat Commun* 8:2214. <https://doi.org/10.1038/s41467-017-02363-w>
- Chang P, Coughlin M, Mitchison TJ (2005) Tankyrase-1 polymerization of poly(ADP-ribose) is required for spindle structure and function. *Nature Cell Biol* 7:1133–1139. <https://doi.org/10.1038/ncb1322>
- Chang P, Coughlin M, Mitchison TJ (2009) Interaction between Poly(ADP-ribose) and NuMA contributes to mitotic spindle pole assembly. *Mol Biol Cell* 20:4575–4585. <https://doi.org/10.1091/mbc.e09-06-0477>
- Cheung M-S, Maguire ML, Stevens TJ, Broadhurst RW (2010) DAN-GL: a Bayesian inferential method for predicting protein backbone dihedral angles and secondary structure. *J Magn Reson* 202:223–233. <https://doi.org/10.1016/j.jmr.2009.11.008>
- Chi NW, Lodish HF (2000) Tankyrase is a golgi-associated mitogen-activated protein kinase substrate that interacts with IRAP in GLUT4 vesicles. *J Biol Chem* 275:38437–38444. <https://doi.org/10.1074/jbc.M007635200>
- DaRosa PA, Wang Z, Jiang X et al (2015) Allosteric activation of the RNF146 ubiquitin ligase by a poly(ADP-ribosyl)ation signal. *Nature* 517:223–226. <https://doi.org/10.1038/nature13826>
- DaRosa PA, Klevit RE, Xu W (2018) Structural basis for tankyrase-RNF146 interaction reveals noncanonical tankyrase-binding motifs. *Protein Sci* 27:1057–1067. <https://doi.org/10.1002/pro.3413>
- De Rycker M, Price CM (2004) Tankyrase polymerization is controlled by its sterile alpha motif and poly(ADP-ribose) polymerase domains. *Mol Cell Biol* 24:9802–9812. <https://doi.org/10.1128/MCB.24.22.9802-9812.2004>
- Dyneke JN, Smith S (2004) Resolution of sister telomere association is required for progression through mitosis. *Science* 304:97–100. <https://doi.org/10.1126/science.1094754>

- Eisemann T, McCauley M, Langelier M-F et al (2016) Tankyrase-1 ankyrin repeats form an adaptable binding platform for targets of ADP-ribose modification. *Structure* 24:1679–1692. <https://doi.org/10.1016/j.str.2016.07.014>
- Guettler S, LaRose J, Petsalaki E et al (2011) Structural basis and sequence rules for substrate recognition by tankyrase explain the basis for cherubism disease. *Cell* 147:1340–1354. <https://doi.org/10.1016/j.cell.2011.10.046>
- Haikarainen T, Krauss S, Lehtiö L (2014) Tankyrases: structure, function and therapeutic implications in cancer. *Curr Pharm Des* 20:6472–6488. <https://doi.org/10.2174/1381612820666140630101525>
- Hottiger MO, Hassa PO, Lüscher B et al (2010) Toward a unified nomenclature for mammalian ADP-ribosyltransferases. *Trends Biochem Sci* 35:208–219. <https://doi.org/10.1016/j.tibs.2009.12.003>
- Huang S-MA, Mishina YM, Liu S et al (2009) Tankyrase inhibition stabilizes axin and antagonizes Wnt signalling. *Nature* 461:614–620. <https://doi.org/10.1038/nature08356>
- Jia J, Qiao Y, Pilo MG et al (2017) Tankyrase inhibitors suppress hepatocellular carcinoma cell growth via modulating the Hippo cascade. *PLoS ONE* 12:e0184068. <https://doi.org/10.1371/journal.pone.0184068>
- Lehtiö L, Collins R, van den Berg S et al (2008) Zinc binding catalytic domain of human tankyrase 1. *J Mol Biol* 379:136–145. <https://doi.org/10.1016/j.jmb.2008.03.058>
- Li B, Qiao R, Wang Z et al (2016) Crystal structure of a tankyrase 1-telomere repeat factor 1 complex. *Acta Crystallogr F Struct Biol Commun* 72:320–327. <https://doi.org/10.1107/S2053230X16004131>
- Li X, Han H, Zhou M-T et al (2017) Proteomic analysis of the human tankyrase protein interaction network reveals its role in pexophagy. *Cell Rep* 20:737–749. <https://doi.org/10.1016/j.celrep.2017.06.077>
- Lupo B, Vialard J, Sassi F et al (2016) Tankyrase inhibition impairs directional migration and invasion of lung cancer cells by affecting microtubule dynamics and polarity signals. *BMC Biol* 14:5. <https://doi.org/10.1186/s12915-016-0226-9>
- Mariotti L, Templeton CM, Raney M et al (2016) Tankyrase requires SAM domain-dependent polymerization to support Wnt-beta-catenin signaling. *MolCell* 63:498–513. <https://doi.org/10.1016/j.molcel.2016.06.019>
- Mariotti L, Pollock K, Guettler S (2017) Regulation of Wnt/beta-catenin signalling by tankyrase-dependent poly(ADP-ribosylation) and scaffolding. *Br J Pharmacol* 174:4611–4636. <https://doi.org/10.1111/bph.14038>
- Marley J, Lu M, Bracken C (2001) A method for efficient isotopic labeling of recombinant proteins. *J Biomol NMR* 20:71–75
- Morrone S, Cheng Z, Moon RT et al (2012) Crystal structure of a Tankyrase-Axin complex and its implications for Axin turnover and Tankyrase substrate recruitment. *Proc Natl Acad Sci USA* 109:1500–1505. <https://doi.org/10.1073/pnas.1116618109>
- Mosavi LK, Minor DL, Peng Z-Y (2002) Consensus-derived structural determinants of the ankyrin repeat motif. *Proc Natl Acad Sci USA* 99:16029–16034. <https://doi.org/10.1073/pnas.252537899>
- Nagy Z, Kalousi A, Furst A et al (2016) Tankyrases promote homologous recombination and check point activation in response to DSBs. *PLoS Genet* 12:e1005791. <https://doi.org/10.1371/journal.pgen.1005791>
- Pollock K, Raney M, Collins I, Guettler S (2017) Identifying and validating tankyrase binders and substrates: a candidate approach. *Methods Mol Biol* 1608:445–473. https://doi.org/10.1007/978-1-4939-6993-7_28
- Preimesberger MR, Majumdar A, Aksel T et al (2015) Direct NMR detection of bifurcated hydrogen bonding in the α -helix N-caps of ankyrin repeat proteins. *J Am Chem Soc* 137:1008–1011. <https://doi.org/10.1021/ja510784g>
- Riccio AA, McCauley M, Langelier M-F, Pascal JM (2016) Tankyrase sterile α motif domain polymerization is required for its role in Wnt signaling. *Structure* 24:1573–1581. <https://doi.org/10.1016/j.str.2016.06.022>
- Riffell JL, Lord CJ, Ashworth A (2012) Tankyrase-targeted therapeutics: expanding opportunities in the PARP family. *Nat Rev Drug Discov* 11:923–936. <https://doi.org/10.1038/nrd3868>
- Sbodio JI, Chi N-W (2002) Identification of a tankyrase-binding motif shared by IRAP, TAB182, and human TRF1 but not mouse TRF1. NuMA contains this RXXPDG motif and is a novel tankyrase partner. *J Biol Chem* 277:31887–31892. <https://doi.org/10.1074/jbc.M203916200>
- Seimiya H, Muramatsu Y, Smith S, Tsuruo T (2004) Functional subdomain in the ankyrin domain of tankyrase 1 required for poly(ADP-ribosylation) of TRF1 and telomere elongation. *Mol Cell Biol* 24:1944–1955. <https://doi.org/10.1128/MCB.24.5.1944-1955.2004>
- Smith S, de Lange T (2000) Tankyrase promotes telomere elongation in human cells. *Curr Biol* 10:1299–1302. [https://doi.org/10.1016/S0960-9822\(00\)00752-1](https://doi.org/10.1016/S0960-9822(00)00752-1)
- Smith S, Giriati I, Schmitt A, de Lange T (1998) Tankyrase, a poly(ADP-ribose) polymerase at human telomeres. *Science* 282:1484–1487
- Troilo A, Benson EK, Esposito D et al (2016) Angiomotin stabilization by tankyrase inhibitors antagonizes constitutive TEAD-dependent transcription and proliferation of human tumor cells with Hippo pathway core component mutations. *Oncotarget* 7:28765–28782. <https://doi.org/10.18632/oncotarget.9117>
- Vranken WF, Boucher W, Stevens TJ et al (2005) The CCPN data model for NMR spectroscopy: development of a software pipeline. *Proteins* 59:687–696. <https://doi.org/10.1002/prot.20449>
- Vyas S, Matic I, Uchima L et al (2014) Family-wide analysis of poly(ADP-ribose) polymerase activity. *Nat Commun* 5:4426. <https://doi.org/10.1038/ncomms5426>
- Wang W, Li N, Li X et al (2015) Tankyrase inhibitors target YAP by stabilizing angiomotin family proteins. *Cell Rep* 13:524–532. <https://doi.org/10.1016/j.celrep.2015.09.014>
- Wishart DS, Sykes BD (1994) The C-13 chemical-shift index—a simple method for the identification of protein secondary structure using C-13 chemical-shift data. *J Biomol NMR* 4:171–180
- Xu D, Liu J, Fu T et al (2017a) USP25 regulates Wnt signaling by controlling the stability of tankyrases. *Genes Dev* 31:1024–1035. <https://doi.org/10.1101/gad.300889.117>
- Xu W, Lau YH, Fischer G et al (2017b) Macrocyclized extended peptides: inhibiting the substrate-recognition domain of tankyrase. *J Am Chem Soc* 139:2245–2256. <https://doi.org/10.1021/jacs.6b10234>
- Yang E, Tacchelli-Benites O, Wang Z et al (2016) Wnt pathway activation by ADP-ribosylation. *Nat Commun* 7:11430. <https://doi.org/10.1038/ncomms11430>
- Yeh T-YJ, Sbodio JI, Tsun Z-Y et al (2007) Insulin-stimulated exocytosis of GLUT4 is enhanced by IRAP and its partner tankyrase. *Biochem J* 402:279–290. <https://doi.org/10.1042/BJ20060793>
- Zhang Y, Liu S, Mickanin C et al (2011) RNF146 is a poly(ADP-ribose)-directed E3 ligase that regulates axin degradation and Wnt signalling. *Nat Cell Biol* 13:623–629. <https://doi.org/10.1038/ncb2222>
- Zhong L, Ding Y, Bandyopadhyay G et al (2016) The PARsylation activity of tankyrase in adipose tissue modulates systemic glucose metabolism in mice. *Diabetologia* 59:582–591. <https://doi.org/10.1007/s00125-015-3815-1>